ELSEVIER

Biophysical Chemistry 128 (2007) 19–29

Biophysical Chemistry

http://www.elsevier.com/locate/biophyschem

Estimation of Förster's distance between two ends of Dps protein from mycobacteria: Distance heterogeneity as a function of oligomerization and DNA binding

Rakhi Pait Chowdhury, Dipankar Chatterji *

Molecular Biophysics Unit, Indian Institute of Science, Bangalore 560012, India

Received 19 February 2007; received in revised form 23 February 2007; accepted 27 February 2007
Available online 2 March 2007

Abstract

Dps protein (DNA binding Protein from Starved Cells) from *Mycobacterium smegmatis* (Ms-Dps) is known to undergo an *in vitro* irreversible oligomeric transition from trimer to dodecamer. This transition helps the protein to provide for bimodal protection to the bacterial DNA from the free radical and Fenton mediated damages in the stationary state. The protein exists as a stable trimer, when purified from *E. coli* cells transformed with an over-expression plasmid. Both trimer as well as dodecamer are known to exhibit ferroxidation activity, thus removing toxic hydroxyl radicals *in vivo*, whereas iron accumulation and non-sequence specific DNA binding activity are found in dodecamer only. This seems to be aided by the positively charged long C-terminal tail of the protein. We used frequency domain phase-modulation fluorescence spectroscopy and Förster Resonance Energy Transfer (FRET) to monitor this oligomeric switch from a trimer to a dodecamer and to elucidate the structure of DNA–Dps dodecamer complex. As Ms-Dps is devoid of any Cysteine residues, a Serine is mutated to Cysteine (S169C) at a position adjacent to the putative DNA binding domain. This Cysteine is subsequently labeled with fluorescent probe and another probe is placed at the N-terminus, as crystal structure of the protein reveals several side-chain interactions between these two termini, and both are exposed towards the surface of the protein. Here, we report the Förster's distance distribution in the trimer and the dodecamer in the presence and absence of DNA. Through discrete lifetime analysis of the probes tagged at the respective regions in the macromolecule, coupled with Maximum Entropy Method (MEM) analysis, we show that the dodecamer, upon DNA binding shows conformational heterogeneity in overall structure, perhaps mediated by a non-specific DNA–protein interaction. On the other hand, the nature of DNA–Dps interaction is not known and several models exist in literature. We show here with the help of fluorescence anisotropy measurements of labeled DNA having different length and unlabeled native dodecameric protein that tandem occupation of DNA binding sites by a series of Dps molecules perhaps guide the tight packing of Dps over DNA backbone.

Keywords: *M.smegmatis* Dps; DNA binding; Fluorescence lifetime; Anisotropy; Rotational correlational time; FRET

1. Introduction

One of the major outcome during evolution of life was the utilization of molecular oxygen from atmosphere instead of other oxidants generated from respiratory or fermentation processes. On the flip side, this advantage turned out to be deleterious at times due to the unavoidable production of reactive oxygen species (ROS) which can damage the biological macromolecules irreversibly, particularly the DNA molecule. In order to prevent such free radical mediated damages, different organisms adopt different pathways, and bacteria offer a plethora of adaptive responses which are very interesting to

Abbreviations: PAGE, Poly Acrylamide Gel Electrophoresis; MLP, Mono Labeled Protein; DLP, Doubly Labeled Protein; HEPES, 4-(2-Hydroxyethyl) Piperazine-1-ethanesulfonic acid; TCEP, Tris(2-carboxyethyl) phosphine hydrochloride; DTT, Dithiothreitol; IAEDANS, 5-[2-(iodoacetamido) ethylamino] naphthalene-1-sulfonic acid; FITC, Fluorescein Isothiocyanate; ds, double strand; nt, nucleotide; FRET, Förster Resonance Energy Transfer; MEM, Maximum Entropy Method; FPLC, Fast Protein Liquid Chromatography; Da, Dalton; kDa, KiloDalton; kb, kilobasepair.

* Corresponding author. Tel.: +91 80 22932836; fax: +91 80 23600535.
E-mail address: dipankar@mbu.iisc.ernet.in (D. Chatterji).

0301-4622/$ - see front matter © 2007 Elsevier B.V. All rights reserved.
doi:10.1016/j.bpc.2007.02.005

study. DNA binding protein from stationary phase cells (Dps) is a group of such proteins which appears progressively as a function of growth of the bacteria and generally are believed to protect the genetic material upon binding them non-specifically. In addition, however, Dps from different organisms are known to exhibit ferroxidation activity *in vivo*, thus protecting the DNA from oxidative radicals generated by Fenton's reaction. Existence of such a novel protein was first reported in the year 1992 by Kolter's group in starved stationary phase cultures of *E. coli* [1]. In our laboratory the Dps homolog from *Mycobacterium smegmatis* was first discovered and a bimodal protection of DNA was reported [2,3]. Dps proteins are known from many other organisms, Gram-positive or Gram-negative alike, and they show DNA binding as a predominant mode of masking DNA [1–5], although protection of the cells are known, in some cases, without binding to DNA [6–8].

In spite of our knowledge of Ms-Dps from functional [3] as well as structural [4] point of view, some interesting questions still remain elusive with respect to Ms-Dps, in particular, how the DNA binding ability of the protein is manifested in its sequence or the molecular mechanism behind trimer to dodecamer conversion. This work was motivated with the thought that a suitably labeled Ms-Dps with fluorescent tags may help in deciphering its DNA recognition as well as dodecamerization mechanisms through Förster's energy transfer (FRET) and anisotropy measurements. The proximate aim, obviously, is to decipher the mechanism of action of Ms-Dps and its peculiar bimodal action in mycobacteria.

Ms-Dps does not have Cysteine residue in its sequence. Thus, we labeled the protein after mutating the 169th Serine residue to Cysteine and subsequently tagging it with a thiol specific probe 1, 5-IAEDANS. The position 169 was important as it is located at the beginning of the putative DNA binding C-terminal domain of Ms-Dps [3]. The other fluorescent moiety, FITC, was placed at the N-terminal of Ms-Dps and both 1, 5-IAEDANS and FITC form an excellent Förster's pair [10–12]. Finally, phase-modulation technique was used to calculate the lifetimes of the donor [13] and they were also subjected to Maximum entropy Method (MEM) analysis [15,16,20,23] to get distribution of lifetimes. Steady state anisotropy and rotational correlation time measurements, on the other hand, revealed some interesting features of DNA recognition.

2. Materials and methods

2.1. Construction of Cysteine mutation by site directed mutagenesis

Serine169 residue at C-terminal tail of the full-length native unlabeled Ms-Dps protein was mutated to Cysteine by site directed mutagenesis according to the *QuickChange* protocol (Stratagene). pET21b specific reverse primer (5′-CCAACTCAGGTACCTTTCGGGC-3′) and forward primer (5′-GAGGGGCAG*TGT*ACCGAGAAG-3′) containing mutation were used in PCR. The mutation was confirmed by DNA sequencing (University of Delhi, South Campus).

2.2. Purification of the mutant protein

The mutant C-terminal His tagged S169C Ms-Dps, was purified following similar protocol as for the native unlabeled protein [3]. *E. coli* strain BL21 DE3 (pLys) was transformed with the vector Cys-pET-*ms-dps*. These cells were grown at 37 °C in Luria Bertini (LB) medium to an A_{600} of 0.6 and then induced with 1 mM isopropyl-1-thio-β-galactopyranoside. Single step purification was performed using the Qiagen Ni–NTA affinity matrix according to the manufacturer's instructions. The purity of the protein was checked on a 12% SDS-polyacrylamide gel, and then the protein was dialyzed against 50 mM Tris–HCl (pH 7.9), 150 mM NaCl overnight and used for further analysis. Protein concentration was determined by the method of Lowry (1951) [9]. For the formation of the higher oligomer, protein at a concentration of 1 mg/ml was incubated at 37 °C for 12 h in 50 mM Tris–HCl (pH 7.9), 150 mM NaCl [3].

2.3. Modification of the single Cysteine with 5-[2-(2-iodoacetamidoethylamino]-1 naphthalenesulphonic acid, {1,5-IAEDANS}

Covalent modification of single Cysteine residue was carried out at pH 7.9 in 40 mM HEPES-KOH, 50 mM KCl, 0.1 mM EDTA and 5% glycerol. Protein sample was incubated with 5-times molar excess of TCEP [Tris2-(carboxyethyl)phosphine hydrochloride] for 20 min on ice. Then 20-fold molar excess of 1,5-IAEDANS was added to protein solution and incubated for another 1 h at room temperature in dark followed by a further incubation of 12 h at 4 °C under rotation. To stop the reaction a 10 fold molar excess of DTT over IAEDANS was added. The unbound probe was removed by passing the reaction mixture through a PD10 gel filtration column (Biorad). The labeling was checked by measurements of O.D. of the sample at 280 nm for protein ($\varepsilon_{monomer}$=22,190 M^{-1} cm^{-1}) and 336 nm for IAEDANS (ε=6300 M^{-1} cm^{-1}). The labeled protein was checked for its oligomerization, ferroxidation and DNA binding activities.

2.4. Modification of the N-terminus of the IAEDANS labeled S169C Ms-Dps with Fluorescein IsothioCyanate (FITC)

Specific covalent modification of only the free NH_2 group at the N-terminus of S169C Ms-Dps trimer and its IAEDANS labeled derivative were carried out at neutral pH in 40 mM HEPES-KOH (pH 7.4), 50 mM KCl, 0.1 mM EDTA and 5% glycerol. To the dialysed protein solution, 50-fold molar excess of FITC was added. The mixture was then stirred for an hour at room temperature in dark. The unbound probe was then removed by passing the reaction mixture through a PD10 gel filtration column (Biorad). The purified labeled proteins were then subjected to O.D. measurements at 280 nm for the protein and 494 nm for the dye to calculate the expected labeling ratio of dye: protein. The ε values are 22,190 M^{-1} cm^{-1} and 64,000 M^{-1} cm^{-1} for the protein monomer and FITC respectively. Both the proteins were checked for their oligomerization, ferroxidation and DNA binding abilities.

2.5. Fast Protein Liquid Chromatography(FPLC) of the native unlabeled and labeled trimers and dodecamers

Oligomeric status of unlabeled WT and MLP and DLP Dps was carried out through FPLC Superdex 200 HR 10/30 column (Amersham Biosciences) with respect to the set of standards with molecular weights, 669, 440, 232, 140, 66 and 16.95 kDa as shown in Fig. 3a. The buffer used was 50 mM Tris–HCl (pH 7.9, 4 °C), 150 mM NaCl in case of proteins as well as the standards. Apparent molecular weights were determined from a plot of log molecular weight vs $K_{av}=(V_e-V_0)/(V_t-V_0)$; V_e=elution volume, V_t=bed volume of the column (25 ml), V_0=void volume, all in ml (inset Fig. 3a). Either unlabeled, mono or doubly labeled dodecamers did not resolve properly in FPLC column and hence they were later subjected to an open Biogel-A-1.5 (Biorad) column. The X axis in each represent elution volume in ml and Y axis was the absorbance at 280 nm.

2.6. Fluorescence lifetime, anisotropy, rotational correlation time measurements

Steady state excitation and emission spectra acquisition and anisotropy measurements of all the labeled proteins were carried out in a Fluoromax-3 fluorimeter (Jovin Yvon)with a Xe-lamp as an excitation source. For lifetime and time resolved anisotropy decay experiments, time resolved fluorimeter Fluorolog-Tau3 (Jovin Yovon) was used, using Phase and Modulation technique, which is a frequency domain method (also known as harmonic method) of measuring lifetime(τ) and rotational correlation time(τ_R). All the fluorescence spectra were source corrected. The experimental curves were finally fitted to the best fit line with least χ^2 value to obtain the lifetime and τ_R values. The theory of Phase and Modulation technique was described in details before [13]. All the experiments were performed at 20 °C.

2.7. Maximum Entropy Method or MEM analysis of lifetime of the donor fluorophore

Several methods are reported in literature to describe distribution of lifetimes [19–23]. However Maximum Entropy Method (MEM) [20,21,23] analysis is different from these methods, as it is independent of any mathematical equation or physical model [23]. Distribution of lifetimes has been obtained by taking the raw lifetime data obtained from a phase-modulation method of discrete lifetime analysis and then executing the programme to get a set of amplitude vs lifetime plots. Later, the peak value, in each plots are taken to calculate the respective set of distances with the help of Förster's equation. Analyses of the data yielded a final lifetime distribution for each sample with respect to the peak value and width of the distribution. Values of χ^2 in the case of a phase-modulation data set should be taken as the least value (best fit), and hence getting a random residual distribution is more important as the value of χ^2 includes the standard deviations of both the phase and demodulation factor. Distances obtained from discrete analysis and MEM analysis agreed well within an error of 1%.

2.8. Distance measurement between the donor and the acceptor by Förster theory

The donor here was 1, 5-IAEDANS labeled at C_{169} position of the C-terminal tail of Ms-Dps protein and the acceptor was FITC, situated at the N-terminus amino acid of the same protein monomer. In Förster's theory of non-radiative dipole–dipole energy transfer [24] the energy transfer efficiency (E) is inversely proportional to the sixth power of the D–A distance given by,

$$R = R_0[(1/E)-1]^{1/6} \tag{1}$$

E can be calculated by either of the following equations,

$$E = 1-Q/Q_0 = 1-\tau/\tau_0 = 1-F_{corr}/F_{0corr} \tag{2}$$

where, Q and Q_0 are the quantum yields, τ and τ_0 are the lifetime values and F_{corr} and F_{0corr} are the corrected fluorescence emission intensities of the donor in the presence and absence of the acceptor respectively.

The Förster critical distance (R_0) is the distance at which 50% energy transfer takes place between D and A and is given as,

$$R_0 = 9.79 \times 10^3[(J)Q(n^{-4})(\kappa^2)]^{1/6} \tag{3}$$

where n is the refractive index of the medium in between D and A and was approximately taken to be equal to 1.4. J is the spectral overlap integral between the emission spectrum of the donor and the absorption spectrum of the acceptor and was given by the following expression,

$$J(M^{-1}\ \mathrm{cm}^3) = \frac{\int F_d(\lambda)\varepsilon_a(\lambda)\lambda^4 d\lambda}{\int F_d(\lambda)d\lambda} \tag{4}$$

where $F_d(\lambda)$ and $\varepsilon_a(\lambda)$ are the fluorescence emission intensities of the donor and molar extinction coefficient (M^{-1} cm^{-1})of the acceptor respectively. λ is the wavelength at a definite nanometer interval. The J value is calculated by using a small FORTRAN programme [33]. In the measurement of R_0 as one of the protein is the estimation of the correct value of κ^2, the orientation factor of the donor and acceptor dipoles. Depending upon the relative orientation of donor and the acceptor the value ranges from 0 to 4. Since the distance is dependent on the sixth root of this value hence variation in the κ^2 value results in only 26% error in R. κ^2 is generally assumed to be equal to 2/3 taking into account that there is a random rotational diffusion of the donor as well as the acceptor prior to energy transfer [17]. However as in our case the lifetime value of the donor (in the protein bound form) is less than its rotational correlation time (also in the protein bound form) in either presence and absence of acceptor (see Results), a range of static D–A orientations are assumed which are remaining unchanged during the lifetime of the excitation. Previously it has been reported [33] that if the donor molecule can be taken as a metal ion, then due to the degeneracy of the higher energy orbitals of metal, randomization of the donor emission can happen during energy transfer and a value of 2/3 for κ^2 is reasonable. However, such is not the

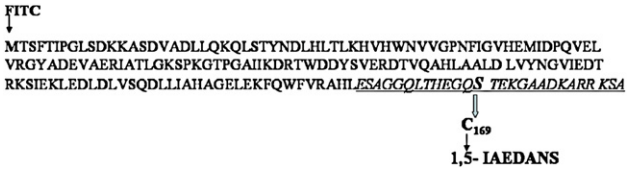

Fig. 1. Schematic representation of fluorophore labeling procedure in single Cysteine mutant of *M. smegmatis* Dps. The Cys169 mutated residue (indicated by the block arrow) has been covalently tagged to Cysteine specific probe 1, 5-IAEDANS followed by modification of N terminal Methionine (M) with FITC. The last 27 amino acid residues in italics (underlined) is the C-terminal tail of Dps.

case here and therefore we estimated distance between the D–A pair with restricted κ^2 value of 0.476 [35,39], assuming a static model of FRET. In addition, in our case diffusion controlled collision between the D–A pair is also unlikely as both the fluorophores are bound to two different sites in the macromolecule, and hence the possibility of having freely diffusing fluorophores is minimum. It should be reemphasized again here, that orientation factor has sixth root dependence in R_0 estimation and thus does not influence the data very much (checked by taking $\kappa^2 = 2/3$, data not shown).

3. Results

3.1. Labeling of Ms-Dps and temperature induced oligomerization of the labeled proteins

Members of the Dps family of proteins are known to form multimers and we have reported sometime back the temperature induced oligomerization of Dps protein from *M. smegmatis* [2]. This transition, as we noticed, was due to a conversion from a trimer to a dodecamer and the structure of the dodecamer was also elucidated at 3.2 Å resolution [4]. One of the most important attribute of Ms-Dps is that the trimer does not bind DNA as opposed to the dodecamer. The sequence analysis of Ms-Dps, as shown in Fig. 1, indicated that there is no Cysteine

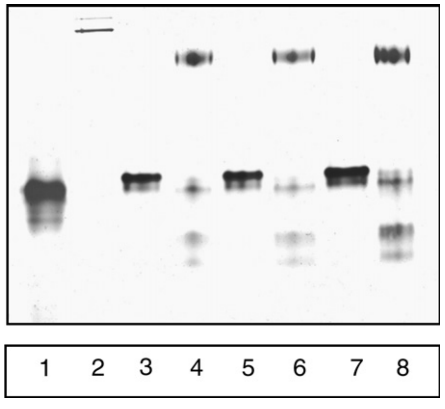

Fig. 2. 10% native PAGE analysis of *M. smegmatis* Dps. Temperature induced oligomerization of the mono and doubly labeled(MLP and DLP respectively) Dps proteins at 37 °C. BSA (*lane1*),Horse Spleen Ferritin (*lane2*), MLP at 4 °C (*lane 3*), MLP at 37 °C (*lane4*), DLP at 4 °C (*lane5*), DLP at 37 °C (*lane6*), native unlabeled Dps at 4 °C *(lane7*), and at 37 °C (*lane 8*). It should be noted here that the standards and Dps have their pI's in the same range.

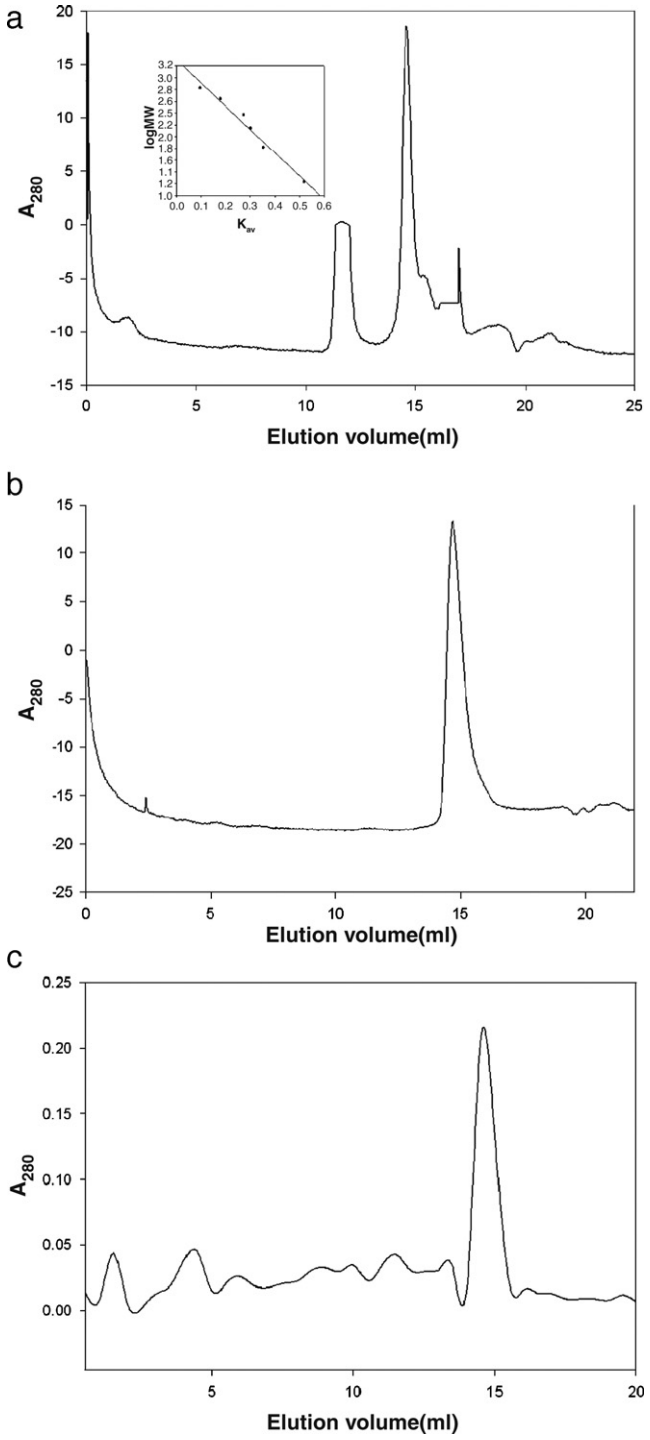

Fig. 3. Determination of the oligomerization status of MLP and DLP Dps through FPLC Superdex 200 column with respect to the set of standards (inset; molecular weights, 669, 440, 232, 140, 66 and 16.95 kDa as shown in a. (a) Native Unlabeled Dps in FPLC column, (b) MLP-Dps, IAEDANS labeled protein at 4 °C in FPLC, (c) DLP–Dps, IAEDANS-FITC labeled at 4 °C in FPLC column. Please note that either unlabeled, mono or doubly labeled dodecamers did not resolve properly in FPLC column. The *X* axis in each represent elution volume in ml and *Y* axis was the absorbance at 280 nm.

in the native protein, and the C-terminal of Ms-Dps is rich in positively charged amino acids. The X-ray structures of the whole protein [4] as well as that of a C-terminal deleted

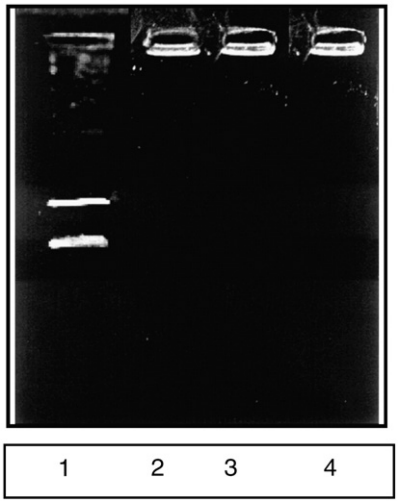

Fig. 4. DNA binding ability of MLP and DLP Dps with non-specific pUC19 DNA. pUC19 DNA alone (*lane1*), pUC19 DNA treated with native unlabeled Dps (*lane2*), IAEDANS labeled Dps *(lane3*) IAEDANS-FITC labeled Dps (*lane 4*); (DNA:protein molar ratio $1:10^3$ in each case, proteins were all incubated to 37 °C prior to incubation with DNA).

derivative of Ms-Dps (unpublished) clearly showed that the C-terminal of Ms-Dps is responsible for DNA binding. We selected the Serine residue at 169th position, critically placed before the DNA binding C-terminal domain as a residue to be mutated to Cysteine, so that a thiol specific probe can be attached (Fig. 1). This probe, 1, 5-IAEDANS acted as a donor fluorophore, whereas FITC at the N-terminal acted as an acceptor. Fig. 2 shows that Ms-Dps when singly labeled with the probe IAEDANS (Mono Labeled Protein; MLP) or doubly labeled with IAEDANS-FITC (Doubly Labeled Protein; DLP), undergo oligomerization as the unlabeled native Ms-Dps and thus, it would be convenient to study the Förster's distance between the donor–acceptor pair.

It should be mentioned here that all the proteins were His_6-tagged at the C-terminal end and they did not interfere with the oligomerization. We also used non-thiolic reducing agent TCEP, during isolation of the trimer. All the estimation showed that the labeling proceeded with molar ratio between probe and the protein as 1:1. Similarly, the molar ratio between IAEDANS and FITC (donor:acceptor) was also found to be 1:1.

In order to confirm further the oligomeric status of the native and labeled proteins, we carried out gel filtration chromatography as reported in Fig. 3. This confirmed the oligomeric status of the proteins as reported by native PAGE analysis. We also observed that the DNA binding ability of the native Ms-Dps or its MLP and DLP derivatives are similar on a 1% agarose gel with non-specific plasmid DNA of defined length (Fig. 4).

Another biological function of the labeled Ms-Dps, ferroxidation activity, was checked before we began our fluorescence analysis, and found to be same as that of the native protein (data not shown). We monitored this activity by following the change in UV absorbance at 305 nm for Fe^{3+}.

3.2. Fluorescence studies: steady state anisotropy and rotational correlation time measurements

We mentioned earlier that the main aim of this study was to probe the change in conformation in Dps as a function of its conversion from a trimer to a dodecamer and the mode of interaction between the dodecamer and DNA. Thus, steady state anisotropy experiments were performed with both the trimer and the dodecamer of Dps in the absence and the presence of pUC19 DNA (2.9 kb) at 10^3:1 molar ratio of protein: DNA for mono and doubly labeled proteins. This amounts to about six phosphate groups or little more than half-a-turn of B-DNA per protein molecule considering 1 μg/ml of DNA is equivalent to 3 μM of phosphate [14]. As can be seen from Table 1A, the anisotropy (r) of the C-terminal probe IAEDANS increased significantly in both MLP and DLP dodecamers when incubated with pUC19 DNA, which indicated the binding of DNA through the C-terminal tail. This binding resulted in a hindered or restricted motion of the fluorophores attached to it. The lifetime and the time-resolved anisotropy decay experiments were performed and the experimentally measured phase shift and modulation data were fitted to a two component and one component model [13], respectively, to get the lifetime and the rotational correlation time values of the fluorophore. We have fitted the rotational correlation time to a single component value, although one may expect a shorter component associated

Table 1A
Average lifetime ($<\tau>$), steady state anisotropy (r) and rotational correlation time (τ_R) values of IAEDANS in MLP (IAEDANS-labeled) and DLP (IAEDANS-FITC labeled) trimer, dodecamer in the absence and the presence of pUC19 DNA

Sample	$<\tau>$ ns	$^*r_{measured}$	τ_R (ns)		r_{calc}	
			One component fit	Two component fit	One component fit	Two component fit
MLP(T)	12.1	0.05±0.01	76.6±5	72.2±2; 1.32±1	0.22±0.05	0.21±0.02; 0.02±0.01
MLP(D)	11.1	0.07±0.01	177.0±2.5	167.5±2; 2.32±1	0.23±0.025	0.23±0.02; 0.05±0.01
MLP(D)+DNA	11.9	0.21±0.03	231.5±5	220.0±3; 4.09±1	0.21±0.05	0.21±0.03; 0.06±0.01
DLP(T)	8.2	0.03±0.02	67.0±5	60.2±4; 0.98±1	0.26±0.01	0.26±0.02 0.03±0.01
DLP(D)	8.5	0.08±0.005	180.0±3	192.0±2; 3.2±1	0.28±0.01	0.29±0.01 0.08±0.01
DLP(D)+DNA	9.3	0.29±0.01	258.0±5	248.0±5; 3.5±2	0.28±0.02	0.22±0.03 0.08±0.01

$^*r_{measured}$ is the steady state anisotropy value of IAEDANS, $r = Ivv - Ivh / Ivv + 2Ivh$.
Ivv is the observed emission intensity when polarizer is oriented parallel to the direction of polarized excitation (Iv, along Z axis), and Ivh is that when the polarizer orientation is perpendicular to the polarized excitation.
(T) and (D) represents trimer and dodecamer respectively.

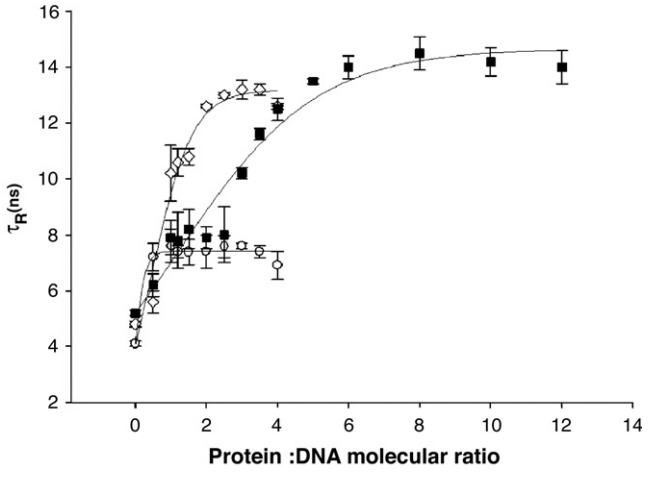

Fig. 5. Variation of rotational correlation time (τ_R) of 5′-fluorescein in 10, 50 and 100 bases long synthetic oligonucleotides after binding to native unlabeled Dps dodecamer in varying molecular ratios : 10 nt (open circle), 50 nt (open diamond), 100 nt (square) ds-DNA binding to protein and saturating at increasing Protein:DNA molecular ratios.

with the free segmental motion of the fluorophore with respect to the macromolecule and the longer one may represent either the domain movement or the overall tumbling dynamics [16]. This became rather apparent when the same data was analyzed with, a two-exponential model and we observed the presence of a shorter component associated with perhaps, the wobbling motion of IAEDANS (Table 1A). However the fractional contribution due to the shorter component in any of the cases were not more than 10%. Average anisotropy value (r_{calc}) shown in Table 1A was estimated from Perrin equation [$r = r_0/(1+\tau/\tau_R)$]. Here "r_0" stands for the maximum anisotropy in the absence of any depolarization and was measured from the experimental data with the fixed lifetimes and "τ" was taken as the average lifetime values as given in Table 1A, whereas "τ_R" was estimated from both one component and two component fits. Therefore, in the case of one component fit, we obtained a single "r_{calc}" whereas two "r_{calc}" were estimated with "τ_R" from two component fit (Table 1A). However, the shorter component is less that 10% of the longer one and our conclusion that the Dps protein showed restricted mobility in the presence of DNA was mainly drawn from the change in "τ_R" in the longer component value. Experimentally measured r average values ($r_{measured}$, Table 1A) of the probe IAEDANS further illustrated the fact that the C-terminal tail in the trimer as well as in the dodecamer retained its flexibility showing always a lower average anisotropy, whereas it approached towards r_{max} (0.4) [17] implicating thereby a rigid C-terminal tail upon binding to the DNA. On the other hand, τ_R showed roughly 100 ns increase on going from a trimer to a dodecamer in MLP and DLP, however, around 54 to 78 ns increase was noticed upon binding to a supercoiled plasmid. Such shifts in the values did explain the oligomerization process of a 63 kDa protein to a 257 kDa protein. However, on an average only a 60 ns increase upon DNA binding probably indicated that due to the positioning of the DNA binding tail at the surface of an almost spherical dodecamer [4], perturbation in the rotational motion of the fluorophore was localized over the surface. DNA binding is not altering the tumbling of the large sphere to a significant extent. It should be mentioned here that such long τ_R values were noticed before too [18]. The significance of this large "τ_R" and its effect on distance measurement will be discussed later.

Dps constitutes a family of proteins that protects DNA in starved bacterial cells via the formation of Dps–DNA co-crystalline complexes *in vivo*. Ren et al. [5] proposed a model for Dps–DNA interaction, depicting formation of a packed, well-ordered, multilayered structure by Dps dodecamers. This observation suggested that DNA was packed between Dps dodecamers in a linear mode through the channels formed between the internal layers. Previously, Grant et al. [6] solved the crystal structure of *E. coli* Dps1 and proposed that the dodecamers pack in pseudo-hexagonal sheets, where a monomer in the unit cell interacts with each of the N-terminus of another monomer and the lysine residues are responsible for DNA binding.

We attempted to understand the DNA–Dps interaction further with the help of fluorescence anisotropy measurements. First, we used a 2.9 kb plasmid pUC19 for the DNA binding studies and monitored the changes in fluorescence parameters like lifetime, r, τ_R of the extrinsic fluorophores IAEDANS tagged at the 169th Cysteine residue in the C-terminal stretch. We used the varying plasmid DNA: protein molar ratio and monitored the r and τ_R values of IAEDANS as a function of DNA–protein interaction. Our gel retardation analysis revealed that at a molar ratio of 1:1000 between DNA: protein, maximum binding takes place (Fig. 4). A molar ratio of 1:1000 can be represented as 1 protein molecule per six phosphate groups of a plasmid DNA, pUC19, of 2.9 kb length. We have mentioned before that 1 μg/ml of DNA is equivalent to 3 μM of phosphate. We have found that the change in anisotropy also saturates around this ratio for both MLP and DLP dodecamer derivatives in the presence of DNA. Changes in τ_R of the fluorophore follows the same pattern in the presence of DNA. The approximate "K_d" calculated seems to be little less that 1 μM, for stoichiometric binding between DNA and Dps.

In the next set of experiments, DNA of varying lengths labeled with fluorescein at the 5′-end (Sigma) were taken and r and τ_R values of fluorescein as a function of DNA: protein molar ratio were estimated. DNA samples were hybridized with the complementary strand prior to any fluorescence measurements and the formation of double strand was assayed following the decrease in A_{260} values. It can be seen from Fig. 5 that upon complex formation, τ_R saturates at various ratios of DNA: protein, as a function of DNA length, indicating that the accessibility of the DNA surface to proteins increases with the length of the DNA. We are tempted at this point to conclude that a tandem, linear model of DNA occupancy by Dps [5] and we will discuss it further in the discussion section. All the fluorescence titration experiments reported above were performed at 20 °C and DNA was incubated with the labeled mutant or native unlabeled dodecamers at 37 °C for 30′ prior to data acquisition.

Table 1B
Calculation of quantum yields (Q) and spectral overlap integral (J) of trimer, dodecamer and DNA bound dodecamer of labeled mutants of Dps

Quantum yields	Trimer	Dodecamer	Dodecamer+DNA
Q_R^*	0.5		
Q_0	0.5	0.5	0.4
Q	0.3	0.2	0.2
$J*10^{-13}$(M^{-1} cm^3)	2.7	3.0	3.5

* Q_R is the quantum yield of the standard quinine sulphate in 0.1 M H_2SO_4.

3.3. Förster Resonance Energy Transfer (FRET) in labeled protein, in the presence and absence of DNA

Corrected fluorescence emission of the IAEDANS labeled and absorption spectra of FITC labeled Dps oligomers were acquired. Emission from the donor (D) near 490 nm overlapped (not shown) to a good extent with excitation of the acceptor (A) near 494 nm, yielding a calculated J (as per Eq. (4)) value $\sim 3*10^{-13}$ M^{-1} cm^3 and shown in Table 1B. Quantum yields of the donor in the presence and in the absence of the acceptor were calculated to estimate R_0, Förster's critical distance, as described in methods. Same R_0 value was taken for the calculations of FRET efficiency and E (Eq. (2) in methods). A set of corrected fluorescence emission spectra of the donor in the presence of varying molar ratios of the acceptor were acquired for both the trimer as well as the dodecamer. As is evident from Fig. 6a, c, maximum FRET efficiency was found nearly at a 1:1 molar ratio of the D–A pair in each case. A separate set of experiments including sensitization of acceptor emission (Fig. 6b, d), also provided with maximum energy transfer at the same molar ratio. The quenching and/or sensitization were found to be independent of the labeled protein concentration (calculated from A_{280} nm values), which further indicated the absence of any intermolecular energy transfer [22,23]. In order to show that the FRET is not occurring between two protein molecules, differentially labeled with a donor and an acceptor, we selected a concentration of the

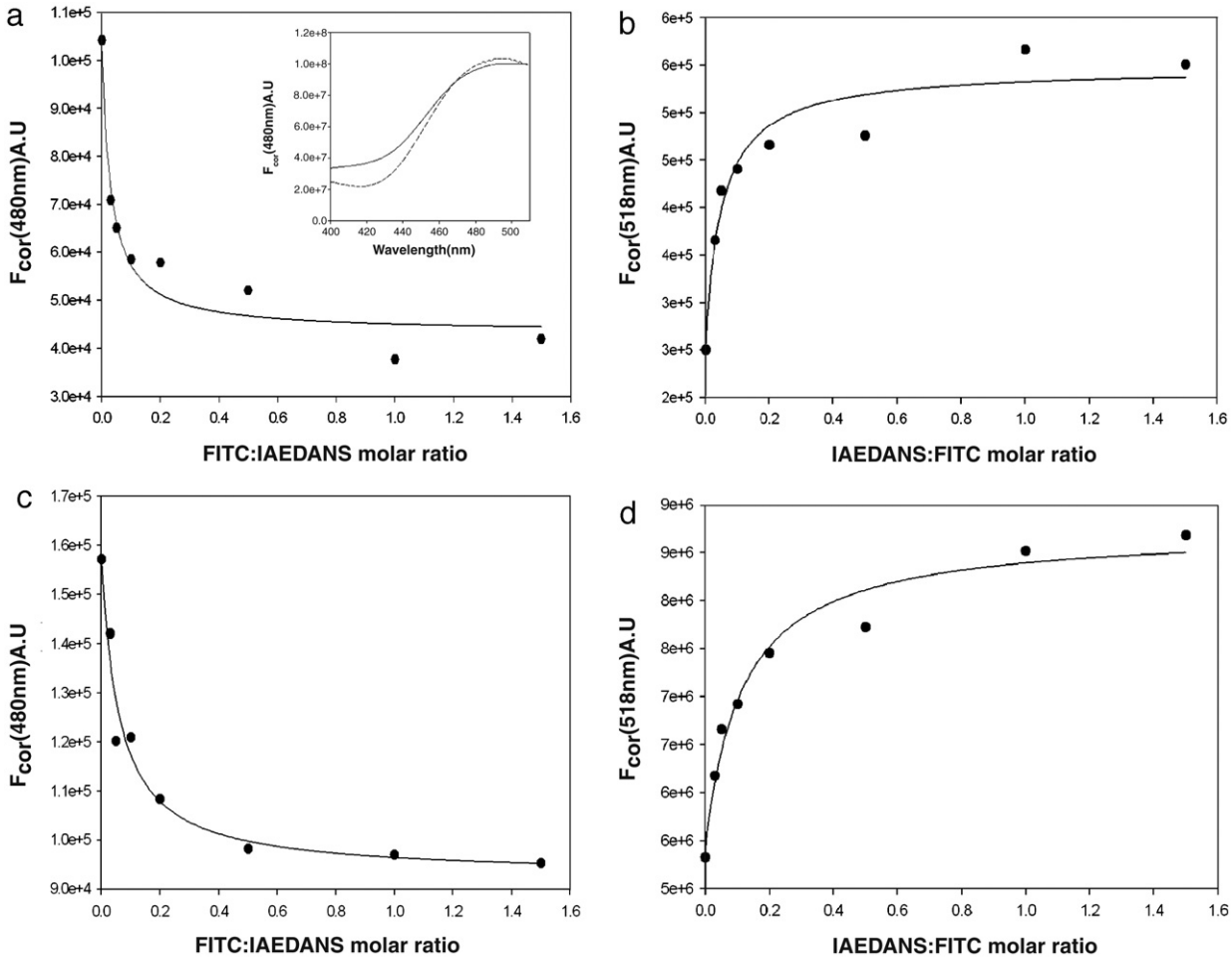

Fig. 6. Quenching of IAEDANS (donor) emission and sensitization of FITC(acceptor) emission in IAEDANS-FITC labeled dodecamers (a, b) and trimers (c, d). Y axis is the corrected fluorescence emission intensity at respective emission maxima (A.U.) as a function of the molar ratio of the donor and acceptor fluorophores. Quenching experiments were performed by taking the donor labeled protein and titrating it with increasing molar ratio of the acceptor FITC, whereas sensitization of the acceptor labeled protein was done separately by titrating it with increasing molar ratio of the donor IAEDANS. Inset in a shows that there is no quenching of fluorescence of the donor IAEDANS in dodecamer (solid line) when equimolar amount of FITC labeled dodecamer (dotted line) was added separately in solution (in presence of DNA), with same protein concentration. Adding increasing amount of the acceptor labeled protein also did not alter the donor fluorescence. Similarly fluorescence enhancement was also not observed when increasing amount of donor labeled dodecamer was added to the solution containing FITC labeled protein initially. The labeled trimers were incubated at 37 °C for 12 h for dodecamerization.

Table 2
Lifetime distribution obtained from discrete exponential fit and MEM analysis

	τ_{trimer} (ns)		$\tau_{dodecamer}$ (ns)		$\tau_{dodecamer+DNA}$ (ns)	
	MLP	DLP	MLP	DLP	MLP	DLP
MEM analysis	16.1	13.8	16.2	11.8	16.2	10.9
	1.4	2.0	1.9	4.8	1.9	0.3
Exponential fit	13.9	8.9	11.9	10.2	14.2	10.3
	2.1	1.7	4.6	1.9	4.5	3.1

protein labeled with donor where it shows maximum quenching when labeled with both donor and acceptor in the same molecule (Fig. 6a). At this concentration of the donor labeled protein a different protein solution was added which is only labeled with the acceptor. Inset of Fig. 6a shows that no quenching of donor fluorescence took place, supporting our contention of intramolecular energy transfer.

3.4. Distance distributions obtained from discrete lifetime values and MEM analysis: a model for structural alterations in the protein upon DNA binding

Förster Resonance Energy Transfer had been extensively used to measure specific distances in labeled macromolecules [34–36]. The extent of energy transfer for a given Donor (D)–Acceptor(A) pair is dependent upon the inverse sixth power of the distances between them. Most measurements of energy transfer, as described by Förster (1948) had been used for estimating specific distances between sites in macromolecules and also to monitor any change in such distances due to various biochemical processes like protein folding [19,22], protein–protein [25–31] and protein–DNA [32] interactions. If a molecule exists in a range of conformations, the ensemble is expected to show a wide range of such distances.

It is known that calculated distances can be erroneous due to the orientation factor κ^2 between the donor and the acceptor as shown in Eq. (3) [36–38] (see Materials and methods). To estimate the value of κ^2 in the case of our system, we observed that in each case $\tau < \tau_R$ (Table 1A), or the fluorophore is not an isotropic rotor during the excited state lifetime or substantial rotation of the molecule cannot occur during its excited lifetime where energy transfer is occurring, suggesting, therefore, a value of κ^2 should be taken as 0.476 rather than 2/3 [33, 35, 39]. However, as there is a sixth root dependence of the distance on the orientation factor, the error with 0.476 or 2/3 is less that 10%.

Fluorescence lifetime acquisition of both the donor and the acceptor in mono and double labeled Dps, in DNA bound and free form were performed using Phase and Modulation Technique [13]. As can be seen from Table 2, the donor showed a multi-component fit even in the absence of the acceptor in all the cases, indicating a multi-exponential decay [13]. Consistent decrease in the donor lifetime in the presence of an acceptor was reflected as a shift towards higher frequency in the experimental graphs. The energy transfer efficiency was calculated from the τ and τ_0 using Eq. (2) (see Materials and methods). Multi-exponential fit generated two lifetimes for donor out of which one is a major/longer component (τ_1; α_1) and the other is minor/shorter (τ_2; α_2). As a standard procedure we decided to measure the Förster's distance from averaging the components ($<\tau> = \tau_1 \alpha_1 + \tau_2 \alpha_2$). Distances obtained are reported in Table 3. It can be seen from the table that all the distances ranged within 50–55 Å (Table 2) and no significant changes were observed. We have also calculated the distance with

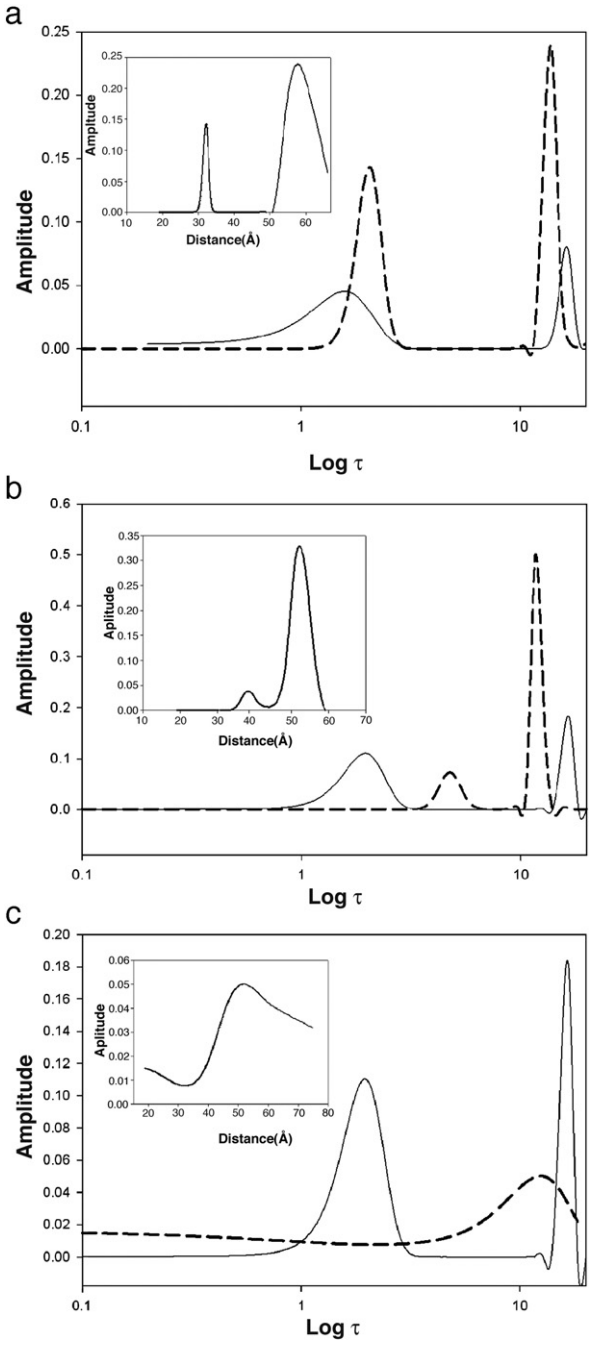

Fig. 7. Fluorescence lifetime distributions of Mono (solid line) and Double labeled (dashed line) Dps trimer (a), Dodecamer (b) and DNA bound dodecamer (c) obtained by Maximum Entropy Method analysis. The *X* axis is fluorescence lifetime in logarithmic space and *Y* axis indicates the amplitude. The inset in each shows the distance distribution plot obtained by converting the lifetime axis to distance using Eqs. (1) and (2) (see Materials and methods).

orientation factor κ^2 taken as 2/3, in both the cases, however, conclusions remained the same.

As we did not measure any change as a function of dodecamerization or upon DNA binding, we subjected the raw fluorescence data of Dps to Maximum Entropy Method (MEM) analysis in order to get the distribution of lifetimes. This method has been used extensively to resolve multiple decay components in time-resolved fluorescence analysis [20,21,23]. Single and multi-exponential decay produce unimodal and multimodal distribution pattern, respectively. The width of the peak(s) in the amplitude vs lifetime plot depends on several factors [15]. One important criterion is the selection of χ^2 value in successive iterations during raw data analysis [15]. Usually, during the iteration that value of χ^2 is selected which yields minimum number of peaks with maximum width for each of them.

In our case, the analysis of raw data as obtained from frequency domain phase-modulation method by MEM was continued till a minimum value of χ^2 was obtained. Fig. 7 shows the final distribution plots of the lifetime of IAEDANS in each case.

Width of the peaks in MEM distribution can be used to interpret the conformational heterogeneity around the fluorophore attached to a macromolecule [15]. We also took into consideration the other parameters which may affect width, like incomplete decay of fluorophore or the signal to noise ratio. The former is not true in our case as at a high frequency employed here, the nanosecond decay will be almost complete. However, for the later case, the true χ^2 value for real time data cannot be estimated and a minimum χ^2 with repeated iterations was the only choice.

It can be noticed from Fig. 7a and b that the nature of the distribution as well as the peak widths associated with the donor (IAEDANS) lifetimes were not significantly changed in the presence of the acceptor. Such was, however, not the case for DLP dodecamer in the presence of the DNA.

In order to obtain the distance map between the donor and the acceptor from lifetime distribution as obtained by MEM analysis (Table 2), one needs a single lifetime of the donor in the absence of the acceptor. However, if the width of the donor lifetime peak in the absence of the acceptor is significantly small, by a factor of 3 or more, in comparison to that in the presence of the acceptor, then it is possible to use the peak value of the donor lifetime. In our case, the width of the major component of the donor lifetime is similar with or without the acceptor. Therefore, the distance distribution obtained from MEM analysis is not very realistic for the protein alone (Fig. 7a, b). On the contrary, in the presence of the DNA (Fig. 7c, Table 4) only a broad single distribution was mapped. This observation led us to propose that in the presence of the DNA, conformational alterations were taken place in the macromolecular surface imposing an altered distance distribution, though a very quantitative heterogeneity prediction here is not possible due to limitation of MEM to analyze raw experimental data.

Table 3
Distance calculations from average lifetime (<τ>) in discrete analysis

	Trimer		Dodecamer		Dodecamer+DNA	
	MLP	DLP	MLP	DLP	MLP	DLP
<τ> (ns)	12.1±0.5	8.2±0.5	11.1±0.5	8.5±0.5	11.9±0.4	9.3±0.4
<R> (Å)	50.4±0.5		54.4±0.5		55.0±0.4	

<R>represents the distance calculated from<τ>.

Table 4
Distances obtained from MEM analysis of the raw lifetime data obtained from phase-modulation method

	Trimer	Dodecamer	Dodecamer+DNA
Distance (Å)	32.5±0.1 60.5±0.3	38.4±0.3 52.1±0.2	52.4±0.2

4. Discussion

Fluorescence spectroscopic studies on C_{169}-IAEDANS labeled as well as both N-terminal-FITC-C_{169}-IAEDANS labeled Ms-Dps protein, showed that, the 27 amino acid residues long C-terminal tail of the protein was flexible in nature and was exposed to the surface; hence was responsible for the DNA binding activity of the protein. This protects the genetic material by physically shielding it from DNA damaging agents. The oligomeric switch from a trimeric species to a dodecamer did not lead to any significant change in overall protein conformation, however, after binding to DNA, as found from the FRET data, all the N–C_{169} distances in each monomer in a dodecameric species was confined to a distance of 50–55 Å. MEM analysis showed that the protein has significant conformational heterogeneity upon binding to DNA, which was not possible to detect from discrete lifetime analysis.

It should be mentioned here that the fluorescent probe attached to the Dps molecule measured a very large rotational correlation time, τ_R. The single component analysis as well as the major part of the double component analysis showed a very high τ_R value. In order to ensure the correctness of this estimation, we measured the steady state anisotropy of the probe and compared it with the values obtained from time-dependent studies. The match between them further confirmed the

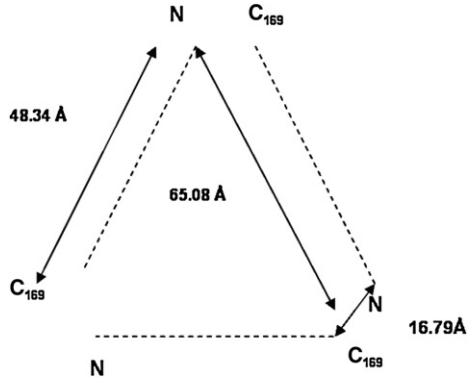

Fig. 8. Schematic representations of the trimeric interface and N–C_{169} distances in a *M. smegmatis* Dps trimer. The dashed line represents the three monomeric chains (A,B,C) in the trimer and the arrows indicate the N–C_{169} distances as obtained from the crystal data of the dodecamer monitored by FRET.

restricted rotation of the probe in the presence of DNA. We observed that binding to Fe (III), results in no change in the overall conformation of Dps, as obtained from both the discrete lifetime and the MEM analysis (data not shown). Though the conformational heterogeneity of the dodecameric species of Dps in the DNA-bound form seems to be interesting and may have remarkable significance in terms of its biological function. Absence of such phenomenon either during ferroxidation or during conformational switch between trimer and dodecamer, add credence to the observation.

One more interesting observation that came out from this study is the tandem binding of Dps on a linear double stranded DNA non-specifically. Our anisotropy saturation data with labeled DNA of varying length support the model proposed by Ren et al. [5].

The above results led us to propose a model satisfying the structural alterations that need to accompany the DNA–Dps complex formation. The trimeric form of Dps has a flexible C-terminal tail exposed to the surface of the protein, and is participating in the Förster energy transfer with the N-terminus, which is also exposed. From the crystal structure of the dodecamer [4], the intramolecular N–C_{169} distances are associated with magnitudes of 16.79, 48.34 and 65.08 Å (Fig. 8). The distances obtained from phase-modulation data are well fitted within this range. It is always expected that the FRET should occur at the smallest distance, but such is not the case here. If there is an actual distance of 16.79 Å in the system then FRET analysis ought to have given that distance. Since we do not get that value, one possible conclusion would be that there is no such short distance in these samples. However, a second possibility is that only those distances falling within ±50% of R_0, 44.5 Å in the present case, can be measured with good precision [40]. MEM analysis of the same phase-modulation data revealed averaging of these distances and two sets of stable distributions were obtained in the trimer as well as in the dodecamer. However, there was a definite change in the value of the distances upon the oligomeric xtransition, which is obvious, as the protein is becoming more compact in the dodecameric form. The interesting point to be noted here is that this flexibility in the overall protein conformation was lost, when the C-terminal tail engaged itself in binding to the DNA in a non-specific manner. The narrow widths associated with the lifetime distributions in case of both trimer and the dodecamer indicate averaging of all the possible orientations/distances between the labeled regions, and no real distance distribution can be predicted. However, in the presence of DNA a realistic, mostly qualitative distance distribution was obtained indicating altered conformational heterogeneity in Dps in the bound form.

Acknowledgements

We thank the Department of Biotechnology, Government of India, for the financial support. RC is supported by the award of a junior research fellow from the Council for Scientific and Industrial research, Government of India. Our sincere thanks to Prof. N. Periasamy, TIFR, Mumbai, for providing the MEMPF programme to get all the distribution plots and Prof. G. Krishnamoorthy, TIFR, Mumbai, for the helpful discussions on this matter.

References

[1] M. Almiron, A.J. Link, D. Furlong, R. Kolter, A novel DNA-binding protein with regulatory and protective roles in starved *Escherichia coli*, Genes Dev. 6 (1992) 2646–2654.
[2] S. Gupta, S.B. Pandit, N. Srinivasan, D. Chatterji, Proteomics analysis of carbon-starved *Mycobacterium smegmatis*: induction of Dps-like protein, Protein Eng. 15 (2002) 503–511.
[3] S. Gupta, D. Chatterji, Bimodal protection of DNA by *Mycobacterium smegmatis* DNA-binding protein from stationary phase cells, J. Biol. Chem. 278 (2003) 5235–5241.
[4] S. Roy, S. Gupta, S. Das, K. Sekar, D. Chatterji, M. Vijayan, X-ray analysis of *Mycobacterium smegmatis* Dps and a comparative study involving other Dps and Dps-like molecules, J. Mol. Biol. 339 (2004) 1103–1113.
[5] B. Ren, G. Tibbelin, T. Kajino, O. Asami, R. Ladenstein, The multi-layered structure of Dps with a novel di-nuclear ferroxidase center, J. Mol. Biol. 329 (2003) 467–477.
[6] R.A. Grant, D.J. Filman, S.E. Finkel, R. Kolter, J.M. Hogle, The crystal structure of Dps, a ferritin homolog that binds and protects DNA, Nat. Struct. Biol. 5 (1998) 294–303.
[7] M. Bozzi, G. Mignogna, S. Stefanini, D. Barra, C. Longhi, P. Valenti, E. Chiancone, A novel non-heme iron-binding ferritin related to the DNA-binding proteins of the Dps family in *Listeria innocua*, J. Biol. Chem. 272 (1997) 3259–3265.
[8] E. Papinutto, W.G. Dundon, N. Pitulis, R. Battistulta, C. Montecnceo, G. Zanotti, Structure of two iron-binding proteins from *Bacillus anthracis*, J. Biol. Chem. 277 (2002) 15093–15098.
[9] O.H. Lowry, N.J. Rosebrough, A.L. Farr, R.J. Randall, J. Biol. Chem. 193 (1951) 265–275.
[10] M. Nyitrai, G. Hild, B. Somogyi, Intermolecular flexibility of Ca- and Mg-actin filaments at different pH values, Eur. J. Biochem. 269 (2002) 842–849.
[11] W. Birmachu, F.L. Nisswandt, D.D. Thomas, Conformational transitions in the calcium adenosinetriphosphatase studied by time-resolved fluorescence resonance energy transfer, Biochemistry 28 (1989) 3940–3947.
[12] K.J. Baker, J.M. East, A.G. Lee, Mechanism of inhibition of Ca2+-ATPase by myotoxin a, Biochem. J. 307 (1995) 571–579.
[13] J.R. Lakowicz, I. Gryczynski, H.C. Cheung, C.K. Wang, M.L. Johnson, N. Joshi, Distance distributions in proteins recovered by using frequency-domain fluorometry. Applications to troponin I and its complex with troponin C, Biochemistry 27 (1988) 9149–9160.
[14] R.F. Schleif, P.C. Wensink, in: Philip Manor (Ed.), Practical Methods in Molecular Biology, Springer–Verlag, New York, 1981, pp. 89–125.
[15] R. Swaminathan, N. Periasamy, Analysis of fluorescence decay by the maximum entropy method: influence of noise and analysis parameters on the width of the distribution of lifetimes, Proc. Indian Acad. Sci., Chem. Sci. 108 (1996) 39–49.
[16] A.M. Saxena, J.B. Udgaonkar, G. Krishnamoorthy, Characterization of intra-molecular distances and site-specific dynamics in chemically unfolded barstar: evidence for denaturant-dependent non-random structure, J. Mol. Biol. 359 (2006) 174–189.
[17] J.R. Lakowicz, Principles of Fluorescence Spectroscopy, Plenum Press, New York, 1983, pp. 112–183.
[18] A. Raghavan, D. Chatterji, Guanosine tetraphosphate-induced dissociation of open complexes at the *Escherichia coli* ribosomal protein promoters *rplJ* and *rpsA* P1: nanosecond depolarization spectroscopic studies, Biophys. Chem. 75 (1998) 21–32.
[19] J.M. Beechem, E. Haas, Simultaneous determination of intramolecular distance distributions and conformational dynamics by global analysis of energy transfer measurements, Biophys. J. 55 (1989) 1225–1236.
[20] J.C. Brochon, Maximum entropy method of data analysis in time-resolved spectroscopy, Methods Enzymol. 240 (1994) 262–311.
[21] R. Swaminathan, G. Krishnamoorthy, N. Periasamy, Similarity of fluorescence lifetime distributions for single tryptophan proteins in the random coil state, Biophys. J. 67 (1994) 2013–2023.

[22] A. Navon, V. Ittah, P. Landsman, H.A. Scheraga, E. Haas, Distributions of intramolecular distances in the reduced and denatured states of bovine pancreatic ribonuclease A. Folding initiation structures in the C-terminal portions of the reduced protein, Biochemistry 40 (2001) 105–118.
[23] G.S. Lakshmikanth, K. Sridevi, G. Krishnamoorthy, J.B. Udgaonkar, Structure is lost incrementally during the unfolding of barster, Nat. Struct. Biol. 8 (2001) 799–804.
[24] T.H. Forster, Intramolecular energy migration and fluorescence, Ann. Phys. (Leipzig) 2 (1948) 55–75. Translated by R. S. Knox.
[25] C.L. Takanishi, E.A. Bykova, W. Cheng, J. Zheng, GFP-based FRET analysis in live cells, Brain Res. 1091 (2006) 132–139.
[26] X. Yang, P. Xu, T. Xu, A new pair for inter- and intra-molecular FRET measurement, Biochem. Biophys. Res. Commun. 330 (2005) 914–920.
[27] H. Wallrabe, H.A. Periasamy, Imaging protein molecules using FRET and FLIM microscopy, Curr. Opin. Biotechnol. 16 (2005) 19–27.
[28] P. Gottfried, M. Kolot, N. Silberstein, E. Yagil, Protein–protein interaction between monomers of coliphage HK022 excisionase, FEBS Lett. 577 (2004) 17–20.
[29] D. Maurel, J. Kniazeff, G. Mathis, E. Trinquet, J. Pin, H. Ansanay, Cell surface detection of membrane protein interaction with homogeneous time-resolved fluorescence resonance energy transfer technology, Anal. Biochem. 329 (2004) 253–262.
[30] V. Levi, F.L.G. Flecha, Reversible fast-dimerization of bovine serum albumin detected by fluorescence resonance energy transfer, Biochim. Biophys. Acta, Proteins & Proteomics 1599 (2002) 141–148.
[31] A.K. Kenworthy, Imaging protein–protein interactions using fluorescence resonance energy transfer microscopy, Methods 24 (2001) 289–296.
[32] S.V. Kuznetsov, A.G. Kozlov, T.M. Lohman, A. Ansari, Microsecond dynamics of protein–DNA interactions: direct observation of the wrapping/unwrapping kinetics of single-stranded DNA around the *E. coli* SSB Tetramer, J. Mol. Biol. 359 (2006) 55–65.
[33] K.P. Kumar, D. Chatterji, Resonance energy transfer study on the proximity relationship between the GTP binding site of *Escherichia coli* RNA polymerase, Biochemistry 29 (1990) 317–322.
[34] L. Stryer, Fluorescence energy transfer as a spectroscopic ruler, Ann. Rev. Biochem. 47 (1978) 819–846.
[35] I.Z. Steinberg, Long-range nonradiative transfer of electronic excitation energy in proteins and polypeptides, Ann. Rev. Biochem. 40 (1971) 83–114.
[36] C.W. Wu, L. Stryer, Proximity relationships in rhodopsin, Proc. Natl. Acad. Sci. U. S. A. 69 (1972) 1104–1108.
[37] R.E. Dale, J. Eisenger, Polarized excitation energy transfer, in: R.F. Chen, H. Edelhoch (Eds.), Biochemical fluorescence, Concepts. Marcel Dekker, Inc., New York, 1975, pp. 115–284.
[38] R.E. Dale, J. Eisenger, W.E. Blumberg, The orientational freedom of molecular probes. The orientation factor in intramolecular energy transfer, Biophys. J. 26 (1979) 161–194.
[39] V. Jain, R.S. Batcha, D. Chatterji, Synthesis and hydrolysis of pppGpp in mycobacteria: a ligand mediated conformational switch in Rel, Biophys. Chem. 127 (2007) 41–50.
[40] A. Bierzyński, Methods of peptide conformation studies, Acta Biochim. Pol. 48 (2001) 1091–1099.